Nature Communications

https://doi.org/10.1038/s41467-026-69728-y

Article in Press

Stratospheric biomass burning aerosols compensate record-breaking ozone depletion over the Arctic in spring 2020

Received: 27 August 2025

Accepted: 9 February 2026

Cite this article as: Zhong, Q., Veraverbeke, S., Yu, P. *et al.* Stratospheric biomass burning aerosols compensate record-breaking ozone depletion over the Arctic in spring 2020. *Nat Commun* (2026). https://doi.org/10.1038/s41467-026-69728-y

Qirui Zhong, Sander Veraverbeke, Pengfei Yu, Jianmin Ma & Shu Tao

Stratospheric biomass burning aerosols compensate record-breaking ozone depletion over the Arctic in spring 2020

Qirui Zhong[1*], *Sander Veraverbeke*[2,3], *Pengfei Yu*[4], *Jianmin Ma*[1], *Shu Tao*[1,5]

[1]College of Urban and Environmental Sciences, Peking University, Beijing, China

[2]Department of Earth Sciences, Vrije Universiteit, Amsterdam, The Netherlands

[3]School of Environmental Sciences, University of East Anglia, Norwich, United Kingdom

[4]College of Environment and Climate, Jinan University, Guangzhou, China

[5]Institute of Carbon Neutrality, Peking University, Beijing, China

*Correspondence to: Qirui Zhong (qrzhong@pku.edu.cn).

Abstract

Biomass burning aerosols reaching the stratosphere (SBBA) present an emerging yet understudied threat to Arctic ozone (O_3). Previous work focuses primarily on SBBA-induced heterogeneous chemistry, while their dynamical effects–altering temperature and circulation–have received less attention. Here, we assess both the chemical and dynamical impacts of SBBA over the Arctic during 2019–2020, a period marked by unusually high SBBA loading and O_3 depletion. With satellite-constrained modelling, we show that SBBA cause a net increase in Arctic O_3, compensating for 19% of the observed depletion in spring 2020. Dynamical processes dominate this effect via stratospheric heating and enhanced poleward O_3 transport. We link this SBBA event to a confluence of northward fire activities and an anomalous polar cyclonic system. Given projected increases in boreal fires and their northward extension, our findings highlight the critical need to integrate both chemical and dynamical SBBA effects to accurately assess O_3 budget and its consequences in a changing climate.

Introduction

Stratospheric ozone (O_3) plays a critical role in Earth's climate and ecosystems[1,2], yet faces an emerging threat from the intensification of large-scale wildfires[3]. Studies have shown that biomass burning aerosols (BBA) in the stratosphere (stratospheric BBA, or SBBA) can deplete O_3 by enhancing chlorine activation[4] and heterogeneous reactions[3,5]. A striking example is the 2019/2020 Australian bushfire, which has led to widespread perturbations in O_3 concentration across the Southern Hemisphere[6,7]. The impact of BBA on O_3 is of particular concern in polar regions, where O_3 variability not only has local impacts but also contributes to broader hemispheric climate feedbacks[8].

Despite recent progress, the effects of SBBA on Arctic O_3 remain poorly understood. While existing studies mostly consider the stratospheric aerosols as volcanic origin, Ohneiser et al. (2021)[9] first report the presence of SBBA in the Arctic. Subsequent studies have demonstrated that SBBA often coincides with O_3 depletion episodes driven by enhanced heterogeneous chemistry[9,10], which is in line with modelling work extensively done for the Antarctic[3,5,6]. However, BBA also serve as an effective climate forcer in the Arctic, posing sizable impacts on radiation budget[11], temperature[12], cloudiness[13], and sea ice coverage[14]. Temperature changes induced by SBBA are particularly relevant for O_3, as Arctic O_3 depletion is strongly linked to the persistence of cold temperatures under a stable polar vortex[15], which triggers a record-high O_3 depletion in spring 2020[16]. Additionally, as Arctic O_3 is strongly affected by the poleward transport of O_3-rich air from lower latitudes via Brewer–Dobson circulation (BDC)[17], any SBBA-driven thermal anomalies might further modulate Arctic O_3 levels by modifying the circulation pattern. The magnitude of SBBA-driven dynamical climate feedbacks on O_3, and how they compare with the heterogeneous chemistry, remain a key barrier in understanding the role of SBBA. Addressing such a gap is essential, especially given projections of increasing wildfire frequencies and aerosol emissions in boreal regions[11,18], which could render the Arctic increasingly vulnerable in terms of O_3 stability.

Here, with satellite-constrained simulations based on CESM2 (the Community Earth System Model 2)[19], we quantify and compare how Arctic O_3 responds to the SBBA from chemical and dynamical perspectives. Our analysis focuses on years 2019 and 2020, when a record-high SBBA loading and O_3 depletion are observed. The presence and impacts of SBBA in this period are further linked with climate anomalies, providing insights into a specific feedback mechanism that affects Arctic O_3 variability via BBA in a warming climate.

Results

Arctic SBBA and O_3 depletion in 2019–2020

According to CALIOP (the Cloud-Aerosol Lidar with Orthogonal Polarization) observations, the stratospheric aerosol optical depth (SAOD) over the Arctic (> 60°N) reaches a peak anomaly of 0.033 during the autumn of 2019 (August–October, Fig. 1a), making the total SAOD more than doubled relative to the multi-year average (0.026, Fig. S1a). Positive anomalies in SAOD are widespread across much of the high-latitude Northern Hemisphere, with the majority of these aerosols confined to the lower stratosphere (below the 100 hPa height, Fig. 1c). Similar anomalies in stratospheric aerosols are also found in 2008 and 2009, which have been attributed to volcanic eruptions[20,21]. Although a volcanic eruption also occurs at middle latitudes (Raikoke, 48.29°N, 153.25°E) in summer 2019[22], field measurements suggest its contribution to Arctic stratospheric aerosol burden is comparatively minor, about an order of magnitude weaker than the signal associated with biomass burning[9,10]. Multiple lines of evidence from satellite observations further support the dominance of SBBA in the 2019 stratospheric aerosol enhancement. Firstly, the Angstrom Exponent (AE)–a parameter describing the spectral dependence of aerosol extinction on wavelength[23]–retrieved over the Arctic during summer 2019 for altitudes between 10–16 km is lower than both the multi-year average (Fig. S2) and values for years with abundant volcanic aerosols (Fig. S3), which agrees with previous studies showing lower AE values when fire smoke dominates over volcanic aerosols[9]. Secondly, measurements from MLS (the Microwave Limb Sounder) do not show SO_2 or sulphate enhancements in 2019 comparable to those observed in 2008 and 2009 (Fig. S4-S5), in line with our model sensitivity simulations which suggest that volcanic emissions are not a major contributor in the 2019 episode (Methods). This is consistent with existing studies demonstrating that the emission from Raikoke eruption is insufficient to explain the large aerosol optical depth at upper troposphere and lower stratosphere (UTLS) in 2019[9,24]. Thirdly, the observed warming at lower stratosphere during summer 2019 indicates the presence of solar-absorbing aerosols such as brown carbon and black carbon (Fig. S6), which is unlikely to be associated with the sulphate heating due to infrared radiation absorption[25] given the low concentration (Fig. S5). The evidence clearly demonstrates the dominance of BBA rather than volcanic aerosols in the Arctic stratosphere.

Following the consistently high SBBA observations in 2019, a record-high O_3 depletion in spring 2020 (February–April) is observed during the past four decades (Fig. 1b). The maximum depletion reaches 78 DU (Dobson units) in March, with 37% of the Arctic areas experiencing a O_3 loss exceeding 100 DU. The depletion is most pronounced in the mid-to-upper stratosphere

according to OMPS (Ozone Mapping and Profiler Suite) observations, with reductions in O_3 of up to 27% at 50 hPa height (Fig. 1d). We identify a significant positive correlation between total column ozone (TCO) and stratospheric temperature at 50 hPa, with 2020 exhibiting the lowest stratospheric temperature on record for the past two decades (-6 ℃, Fig. S7). This anomalously low temperature favours the formation of polar stratospheric clouds (PSC) by threefold compared to a climatology[26] (Fig. S8), and triggers several conditions conducive to heterogeneous chemical reactions, including the chlorine activation via conversion of HCl to ClO (Fig. S9b-S9c) and condensation of HNO_3 into nitric acid trihydrate (NAT, Fig. S9d), both of which facilitate catalytic O_3 destruction[15,16].

While existing studies have primarily attributed the record-breaking Arctic O_3 depletion to dynamical drivers, including weakened wave activity and a suppressed BDC[15,27,28], few have considered the potential impacts of SBBA. Given the sensitivity of O_3 concentration to temperature and the capacity of BBA to perturb both radiative budget and chemical processes, we hypothesise that the 2019 SBBA event plays a role in the observed Arctic O_3 depletion in 2020.

Impacts of Arctic SBBA on O_3 depletion

We employ the CESM2 driven by GFED (Global Fire Emission Database 4s)[29] to investigate the impacts of anomalous SBBA on the O_3 concentration for the 2019–2020 period. To better represent the vertical distribution of SBBA, the fire injection profiles are modified to match satellite observations from CALIOP (see Methods). With this observationally constrained model, we conduct three sets of simulations: two climatological runs from 2000 to 2023 with (CLIM) and without (NOBB) fire emissions, and a 20-member ensemble run (FIRE19) focusing on the specific influence of 2019 fire injections. Paired simulations are conducted for all the three experiments with either the default or updated stratospheric chemistry schemes to fully account for the dynamical and chemical impacts of SBBA (see Methods). By comparing CLIM and FIRE19, we show that the 2019 SBBA overall lead to an Arctic TCO increase by 11.5 DU (-2.8–25.5 DU as interquartile range) during spring 2020. Relative to the 2000-2023 average level, such an increase offsets 19% of the observed O_3 depletion (59 DU).

To disentangle the underlying mechanisms, we separate the SBBA effects on O_3 into chemical (by enhancing heterogeneous reactions and the resulting consequences) and dynamical (by altering temperature and circulation) components by applying varying stratospheric chemistry schemes (see Methods). Our simulations show that SBBA-induced heterogeneous chemistry leads to a TCO reduction of 6.1 DU (10% of the observed depletion) during spring 2020. However, this effect is overwhelmed by a dynamically driven O_3 increase of 17.6 DU (4.4–31.7 DU), resulting in a net

positive anomaly (Fig. S10). Vertical profiles demonstrate that the compensation between the two effects occurs primarily above 100 hPa height, below which the dynamical impacts dominate (Fig. 2b). Strong chemical impacts are found between 10 and 100 hPa level, yielding an average O_3 depletion of 0.09 ppmv. However, the accompanying dynamical impacts produce an O_3 increase that is roughly 50% larger (0.14 ppmv). Consequently, O_3 concentrations rise by a net 0.05 ppmv at this altitude range, contributing substantially to the positive Arctic TCO anomaly. These results suggest that, in the absence of the 2019 SBBA event–particularly the dynamical impacts–Arctic O_3 depletion would have been more severe. While the typical threshold for an O_3 hole is defined by a TCO below 220 DU[30], such values have not been observed in the Arctic on a monthly basis in OMPS dataset. However, our results suggest that without the 2019 SBBA, this threshold would have been exceeded over an area of approximately 1.8×10^4 km^2 in March 2020 (Fig. S11).

Our further analysis reveals that the impacts of SBBA on O_3 arise primarily through their perturbations to local temperature and large-scale circulation. By comparing FIRE19 and CLIM simulations with varied chemistry schemes (Methods), we decompose the SBBA-induced effects into three temporal stages based on the distinct temporal evolution of SBBA, O_3, and climate dynamics. In Stage-1 (July–October 2019) immediately after the SBBA injection, a dense aerosol layer forms below 100 hPa height as also observed by CALIOP (Fig. 1c), resulting in a strong thermal dipole with heating within and weak cooling above the layer (Fig. 3d). Such a dipole structure is induced by the solar absorption of BBA, which cannot be formed in the case of volcanic aerosols as widely studied in previous studies. This initial heating within the aerosol layer increases O_3 by disrupting ice cloud content (Fig. S12) and suppressing chlorine/bromine activation (Fig. S13). MLS and ERA5 data record a similar heating pattern (Fig. S14), which becomes obscured after September, possibly masked by the further changes associated with the rapid polar vortex development[31,32] (Fig. S15). Simultaneously, this thermal structure facilitates upwelling above 200 hPa height (i.e., negative anomalies in residual vertical velocity, Fig. S16) and dilutes O_3-rich air in the middle stratosphere (Fig. 3b1), which is corroborated by OMPS and ERA5 data (Fig. S17). While in Stage-2 (November 2019–January 2020) which marks the onset of the polar vortex (Fig. S18), the lower-stratospheric warming persists, promoting upward wave penetration and leads to an EP flux convergence at upper stratosphere (Fig. S19). This is accompanied by an enhanced poleward O_3 transport via enhanced BDC, as indicated by the tightened residual meridional velocity (Fig. S20). However, this effect is largely overridden by a dominant chemical-radiative feedback loop. The initial chemical O_3 depletion caused by SBBA cools the lower stratosphere (Fig. S21), enhancing vertical stability, suppressing wave penetration, and ultimately weakening the BDC (Fig. S19). This reduced poleward transport synergizes with direct chemical depletion

due to SBBA, leading to a substantial Arctic TCO decline (13.1 DU) in this period. Stage-3 (February–April 2020) sees the dynamical effects re-intensify and become dominant as the background BDC strengthens seasonally. The SBBA-induced strengthening of the BDC enhances poleward O_3 transport and downwelling over the Arctic (Figs. S16, S20), which warms the stratosphere, weakens the polar vortex (Fig. 3e4), and suppresses PSC formation (Fig. S22), driving a net increase in O_3 concentration (Fig. 3a4). Overall, our results highlight that the impacts of SBBA on Arctic O_3 during 2019–2020 are governed more by dynamic feedbacks—particularly via local heating and circulation modulation—than by chemical pathways.

Given that the anomalous climate conditions of spring 2020, characterized by the exceptionally low temperatures and strong polar vortex[15,27,28], can influence O_3 evolution, we additionally perform a hybrid simulation integrating free-running and nudged configurations (see Methods). This framework more accurately reproduces the observed temperature anomalies and O_3 depletion for the focused period (Figs. S23-S24). Importantly, the estimated dynamical and chemical impacts of SBBA derived from this hybrid approach are consistent with those from the free-running simulations discussed above (Fig. S25), which demonstrates that our findings are robust and largely independent of the background climate state. In addition, our results highlight the warming induced by SBBA, which is validated against MLS and ERA5 data. Although aerosol modelling is constrained by CALIOP observations, our modelled warming shows notable overestimation (Fig. S26b-c). To evaluate the potential impacts of such bias, we conduct a sensitivity test by reducing BBA emissions to align the modelled temperature response with observations, which suggests an optimal scaling factor of 0.5 (Methods). A 10-member ensemble using half GFED emissions further indicates a net TCO increase of 5.7 DU (with an interquartile range of −8.7 to 19.5 DU) during spring 2020 (Fig. S26a). This falls well within the uncertainty range of the default GFED-driven simulations, further demonstrating the robustness of our conclusions.

Possible drivers for the 2019 SBBA episode

Given the impacts of SBBA on Arctic O_3, we further investigate the drivers behind the exceptional stratospheric injection of BBA in summer 2019. Field measurements indicate that the SBBA in the Arctic primarily originate from Siberia[9,10], consistent with global emission inventories identifying Siberia as the dominant source of boreal BBA emissions in 2019 (Fig. S27). While intense biomass burning can inject smoke into the UTLS via pyrocumulonimbus activity[33] and self-lifting with sufficient black carbon content[9], the intensity of fires alone cannot explain the anomalous 2019 event. In fact, BBA emissions from Siberia are similar in 2020 and even higher

in 2021 (by 20–90% across multiple inventories) compared with 2019, yet no substantial stratospheric aerosol signal is detected over the Arctic for these years (Fig. 4b). This discrepancy points to additional factors shaping SBBA distributions.

Our analysis reveals that the 2019 fire season is characterized by a unique combination of northward fire occurrence and anomalous atmospheric circulation at UTLS. As shown in Fig. 4a-4b and Fig. S28, satellite observations demonstrate elevated stratospheric aerosol loading during all three selected intense fire years (2019–2021), yet only in 2019 do the aerosols reach the Arctic stratosphere efficiently. In contrast, stratospheric aerosols in 2020 and 2021 remain largely confined to the mid-latitude Westerlies (40–60°N). Such a discrepancy becomes most apparent in July, when the frequency and intensity of Siberian fires peak (Fig. S29). It has been well documented that plumes from intense fire activities can reach the UTLS level by self-lifting, provided sufficient black carbon content and solar radiation[7,9], while the subsequent transport and distribution of these aerosols depend strongly on prevailing circulation patterns. By mapping the spatial distribution of extreme fires in July which are defined as daily fire radiative power exceeding 100 MW per 0.1° grid cell (i.e., approximately top 10% of severity across the boreal zone for the entire 2003–2023 period), we find that over 15% of the extreme fires in 2019 occur northward of 65°N, ranking the second in terms of extreme fire frequency following 2020. Concurrently, there is a pronounced low geopotential anomaly at 300 hPa level developed over the East Siberia, forming a strong cyclone system that enhances vertical motion and poleward transport of aerosols emitted from eastern and northern Siberia (Fig. 4c). In comparison, extreme fires in 2021 are located farther south, and circulation anomalies in 2020 are much weaker. Under such conditions, lofted BBA in 2020 and 2021 are trapped by mid-latitude anticyclonic systems and advected southward and downward into the mid-latitude Westerlies, failing to reach the Arctic stratosphere. Additionally, while we identify numerous extreme fire events during the 2003–2023 period other than 2019–2021, the resulting plumes do not efficiently reach the Arctic stratosphere. This outcome is primarily attributed to the absence of the specific coupling between fire location and atmospheric circulation that is observed in 2019 (Fig. 4f and Fig. S30). This suggests that, beyond fire intensity, the circulation pattern plays an important role in determining the distribution of SBBA at mid-to-high latitude in Northern Hemisphere.

Discussion

In this work, we assess the Arctic O_3 response to SBBA using an observation-constrained model. Different from previous studies that primarily emphasize O_3 loss driven by heterogeneous chemistry, we show that the dynamical consequences triggered by SBBA solar absorption are more

important, which result in a net increase in TCO over the Arctic by enhancing northward O_3 transport from lower latitudes via circulation modulation. Our simulations also reveal that even for chemical impacts, the chemical-dynamical feedback following the O_3 loss plays a more significant role than direct heterogeneous reactions. By comparing these effects with observed O_3 concentration, we estimate the 2019 SBBA injection overall compensates for 19% of the record-breaking O_3 depletion in 2020 spring. These findings suggest that BBA may influence climate not only through direct and indirect radiative effects as widely discussed in previous studies, but also by modulating stratospheric O_3 which is proven to be an efficient driver of hemispheric climate variability[8]. However, such effects become substantial only when significant quantities of BBA reach the Arctic stratosphere, as constrained by satellite observations. Notably, both our default CESM2 simulations and many other global models tend to underestimate the vertical extent of BBA plumes[34,35], which suggests potential biases in the configuration of fire emission injection and plume self-lifting. Therefore, proper representation of BBA vertical transport is critical for accurately quantifying their chemical and climatic impacts in global models.

It has been documented that the observed Arctic O_3 depletion in spring 2020 is coupled with anomalously low temperatures, a feature not fully captured by free-running simulations. By introducing nudging constraints to align modelled meteorology with observations, we confirm that while absolute O_3 concentrations are sensitive to the climate state, the SBBA-induced perturbations remain remarkably consistent with the free-running simulations. This implies that the fundamental mechanisms and the associated impacts of SBBA identified in the present study are generalizable to other stratospheric BBA injection episodes, provided sufficient aerosol loading is present.

Although intense fire activities are prerequisites for aerosols being injected into the stratosphere, our results demonstrate that fire intensity alone cannot fully explain the extreme Arctic SBBA event observed in 2019. We show that the 2019 episode is unique, resulting from a combination of northward distribution of extreme fire activities and an anomalous high-altitude cyclone. The extreme fires facilitate upward transport of smoke plumes, which are subsequently delivered to the Arctic by an anomalous cyclone at UTLS level. Under future climate warming, fire frequency and intensity at the northern boreal edge are projected to increase[18,36,37]. Whether these increased BBA can enter the Arctic stratosphere and potentially affect O_3 budget therefore strongly depends on the high-altitude atmospheric conditions. The interplay between increasing fire activities and future circulation patterns introduces new complexities in understanding how climate change, wildfires, and Arctic O_3 dynamics interact. Further studies are therefore warranted

to quantify the joint probability of these compounding events and their impacts on Arctic O_3 chemistry and dynamics.

While our results demonstrate that the exceptional 2019 Arctic SBBA events can influence Arctic O_3 through both dynamical and chemical pathways, our conclusions are subject to model-related uncertainties. The stratospheric chemistry triggered by SBBA is relatively well constrained in CESM2[4], while the dynamical impacts, particularly those linked to temperature and circulation responses to aerosol and O_3 forcing, remain less certain and vary substantially across global climate models[38,39]. To partially address this, we assess the aerosol climate sensitivity of CESM2 in comparison with other models using historical experiments from the CMIP6 archive (Methods). Driven by identical aerosol emissions, CESM2 produces a moderate Arctic radiative forcing and temperature response that aligns closely with the CMIP6 multi-model ensemble mean (Fig. S31). Nonetheless, aerosol–climate interactions in the stratosphere remain less explored than those in the troposphere, and future model developments are required to address the associated uncertainties. In addition, despite the critical role of SBBA-induced warming on Arctic O_3, our model overestimates this effect when constraining stratospheric aerosol loading with CALIOP observations, which is partly associated with the retrieval uncertainties in CALIOP data[9]. Future efforts should therefore focus on integrating multi-source observations to more robustly constrain SBBA loading and its associated climate response. Moreover, we note that while the 2019 stratospheric aerosol anomaly is primarily attributed to SBBA based on observational evidence, existing studies show that Raikoke eruption might contribute to UTLS aerosol optical depth by 15-30%[9,24], indicating that the impacts of volcanic sulphate cannot be entirely ruled out. However, such estimates remain uncertain, particularly when inferred from various observational datasets[40]. Future studies that integrate multi-platform measurements with observationally constrained modelling will be essential for better understanding the relative contributions of volcanic sulphate co-occurring with the anomalous fire smoke in 2019, thereby contributing to a better understanding on the dynamical and chemical evolution of the Arctic ozone in a changing climate.

Methods

Observational data

This study focuses on the Arctic region (> 60°N) during the period 2000–2023. Observations for stratospheric aerosols and O_3 were mainly obtained from satellite datasets. For aerosols, we used the total extinction profiles and SAOD data from CALIOP[41] (2006–2021, monthly) and OMPS[42] (2012–2023, daily), both of which have been extensively validated in previous studies[41,43]. The SAOD from CALIOP was mainly used to validate model results and was obtained by integrating the monthly mean aerosol extinction coefficients from 1 km below the MERRA-2 (The Modern-Era Retrospective analysis for Research and Applications, version 2) tropopause height to 36 km. The aerosol extinction coefficients (*EC*) at multiple wavelengths (λ) from CALIOP and OMPS were further used to calculate Angstrom Exponent (AE)[23] using equation (1)

$$AE = -\frac{\log(EC_{\lambda_1}/EC_{\lambda_2})}{\log(\lambda_1/\lambda_2)} \quad (1)$$

In addition, we also used MODIS (Moderate Resolution Imaging Spectroradiometer) observations for total aerosol optical depth[44] to independently validate our aerosol injection parameterization in modified simulations. For O_3, the O_3 volume mixing ratio data were taken from SWOOSH (Stratospheric Water and Ozone Satellite Homogenized), which merges multi-source satellite records[45]. TCO for the whole study period was collected from NASA Ozone watch (https://ozonewatch.gsfc.nasa.gov/), which integrates OMPS retrieval and MERRA-2 reanalysis. Gridded TCO data from OMPS were also used to validate model performance. MLS L3 observations of temperature, ClO, HCl, and HNO_3 from 2004 to 2023 were used to further verify our analysis (https://science.nasa.gov/mission/aura/mls). The meteorological data were obtained from ERA5 for circulation analysis[46]. Daily fire radiative power data at 0.1-degree resolution from 2003 to 2023 were obtained from GFAS (the Global Fire Assimilation System), which are originally based on MODIS active fire products[47].

Model configuration and observational constraints

We used the CESM2 (Community Earth System Model version 2.1.3) to study the impacts of SBBA on O_3 concentration. Given our focus on stratospheric processes, we utilized WACCM (Whole Atmosphere Community Climate Model) as the atmospheric component, which includes fully interactive chemistry for both troposphere and stratosphere[48]. All simulations were run at a horizontal resolution of 1.9° latitude × 2.5° longitude with 70 vertical layers stretching from surface to 6×10^{-6} hPa (140 km). Emissions of anthropogenic and biomass burning (BB) sources

were taken from GEMS (Global Emission Modeling System, https://gems.sustech.edu.cn/) and GFED (Global Fire Emission Database 4s, https://www.globalfiredata.org/), respectively. To isolate the impacts of BBA, we fixed anthropogenic emissions to 2010 level for all simulations. The modelled vertical profiles of aerosol extinction at 550 nm over the Arctic were validated against CALIOP observations, showing notable underestimation of stratospheric aerosols using default configuration (Fig. S1). We therefore modified the fire emission profiles by uniformly distributing the BB emission from surface to a prescribed height, while keeping the total emission intensity the same as those in GFED. Sensitivity tests indicated that an injection height of 12 km yielded good agreement with CALIOP profiles for the 2019 fire season, while 5 km provided a reasonable fit for other years (Fig. S1). These modifications also brought models more in line with MODIS observation for total aerosol optical depth, which independently verified our parameterization (Fig. S32). The adjusted emission profiles were applied throughout this study.

As there was a strong eruption at Raikoke volcano (48.3°N, 153.2°E) on 21-22 June 2019 that might potentially affect stratospheric aerosols and O_3, we made paired sensitivity simulations with and without this particular source. The total amounts of SO_2 emissions and vertical profile parameterisation followed Cai et al., 2022[22]. The modelled output demonstrated negligible difference between the two simulations for the Arctic O_3. We therefore excluded the impacts of volcano emissions in our study.

Model experiment setup

To investigate the impacts of SBBA, we designed the following three experiments:

1. CLIM, which was a climatology run from 2000 to 2023 driven by annually varying GFED emissions, with all BB emissions injected from surface to 5 km height. This experiment served as the baseline and represented typical BB conditions. The modelled TCO from CLIM was further validated with observations from OMPS, demonstrating good agreement with OMPS observations in terms of both spatial patterns and seasonal evolution (Fig. S33).
2. FIRE19, which ran successively for 40 years with repeating emissions from 2019 to 2020 (20-member ensemble). The BB emissions in 2019 were injected from surface to 12 km to match observed aerosol profiles (Fig. S1). The difference between FIRE19 and CLIM indicates the impacts of abnormal SBBA seen from observations, which is the core of the present study.
3. NOBB, which was the similar to CLIM except that all BB emissions were switched off.

All the above experiments were initialized from identical initial conditions and were run for 4 years prior to analysis as spin-up. Data for the 24 years from CLIM and NOBB runs were averaged

to provide climatology baseline. Given our focus on the O_3 anomaly induced by the 2019 SBBA event relative to climatological conditions, the core of our analysis centred on the differences between FIRE19 and CLIM simulations.

The default WACCM configuration calculates heterogeneous chemical reaction rates based on aerosol surface area density for three types (sulphate, nitric acid trihydrate, and water-ice aerosols)[48], which, however, does not account for the impacts of BBA. To address this and allow for the separation of effects, we conducted the following paired simulations for the FIRE19, CLIM, and NOBB experiments, leveraging two distinct chemical schemes:

- Default chemistry scheme: fire aerosols did not directly participate in heterogeneous chemical reactions in the stratosphere, so that only the dynamical impacts (e.g., modifications on radiation, temperature, and circulation) were captured.
- Updated chemistry scheme: following Solomon et al. (2023)[4], this scheme allowed organic aerosols to enhance O_3-depleting heterogeneous chemical reactions.

This approach allows us to distinguish the total SBBA influences into two components. The 'dynamical impacts' were quantified by the FIRE19–CLIM results under the default chemistry scheme, primarily reflecting aerosol-induced alterations to temperature and circulation. The 'chemical impacts' were estimated as the difference of FIRE19–CLIM results between the updated and default chemistry schemes, capturing the effects stemming from BBA heterogeneous reactions and the subsequent impacts of O_3 depletion. We note, however, that this partitioning is not absolute due to the inherent interactions between dynamical and chemical processes. For instance, the dynamical effects can modify ice cloud content and PSC formation, which further alters the O_3 chemical loss rate. Conversely, chemical loss of O_3 subsequently leads to changes in temperature via interactions with longwave radiation. Throughout this paper, the terms 'dynamical' and 'chemical' were used to refer to the initial and direct effects of SBBA rather than the overall, non-linear coupled responses.

To better interpret the impacts of SBBA, we divided the focused study period (July 2019–April 2020) into three distinct stages. Stage-1 (July–October 2019) represents the period of high SBBA loading immediately following the aerosol injection. Stage-2 (November 2019–January 2020) is defined as a transition period, coinciding with the initial development of the polar vortex (Fig. S18). Stage-3 (February–April 2020) is the primary focus of this study, during which a record-high Arctic ozone depletion was observed (Fig. 1b).

To account for the anomalous meteorological conditions of spring 2020, we further developed

a hybrid simulation framework. First, a fully nudged simulation towards ERA5 for 2019–2020 was performed to generate realistic initial conditions. For each month from January to April 2020, we then conducted the following three experiments:

1. *Baseline*: A free-running simulation initialized from the nudged state at the end of the previous month.
2. *Perturbed dynamic*: Similar to 'Baseline', but with the initial conditions adjusted to remove the estimated dynamical effects of SBBA from the previous month, as derived from the earlier free-running simulations. Such perturbations were applied to both atmospheric constituents (O_3, aerosols, precursors, etc.) and meteorological fields (temperature, geopotentials, wind, etc.). As our earlier free-running simulations present 20-member ensembles, this perturbated experiment also consisted of 20 ensemble members, with each initialized with the corresponding member.
3. *Perturbed chemistry*: Identical to 'Perturbed dynamic' except that the perturbations reflect the estimated chemical impacts of SBBA rather than dynamical ones.

The deviations of the two perturbated experiments from 'baseline' were then used to quantify the dynamical and chemical impacts of SBBA. This approach disentangled the dynamical and chemical influences of SBBA while maintaining generally realistic meteorological conditions for the focused period (Fig. S23). Note that these experiments were not conducted for 2019, as observations indicated that the temperature and O_3 concentration in 2019 were close to 2000–2023 climatological levels, which were already captured accurately by our free-running simulations (Figs. S23-S24). Given the agreement of the SBBA impacts between the above free runs and this hybrid simulation (Fig. S25), we retain the conclusions derived from the original free-running ensembles.

Our analysis suggested that SBBA-induced impacts on Arctic O_3 were tightly associated with stratospheric aerosol warming. While the initial aerosol simulations were constrained using CALIOP data, comparisons against MLS observations and ERA5 reanalysis revealed an overestimation of the SBBA-induced warming (Fig. S26b-c). To quantify the impacts of this bias, we conducted a series of sensitivity experiments by linearly scaling the BBA emissions from 1.0 down to 0.1, and evaluated the modelled stratospheric temperature response against observed anomalies from MLS for the summer of 2019 (July and August). A scaling factor of 0.5 was determined to yield the optimal agreement between the modelled and observed temperature magnitudes (Figs. S14, S26). Consequently, this factor was applied to the BBA emissions to perform a 10-member ensemble run, which utilized a configuration identical to FIRE19 using

updated chemistry scheme, with the sole exception of the adjusted emission magnitude.

Data Availability

The CALIOP aerosol profile data are available at https://asdc.larc.nasa.gov/project/CALIPSO. OMPS observations can be accessed at https://www.earthdata.nasa.gov/data/instruments/omps. MLS data are available from https://www.earthdata.nasa.gov/data/instruments/mls. MODIS observations can be accessed at https://modis.gsfc.nasa.gov/data/dataprod/mod08.php. SWOOSH data can be obtained from https://csl.noaa.gov/groups/csl8/swoosh/. MERRA2 data can be downloaded from https://gmao.gsfc.nasa.gov/gmao-products/merra-2, TROPESS reanalysis data are available at https://disc.gsfc.nasa.gov/. ERA5 data are accessed from https://cds.climate.copernicus.eu/. Fire radiative power from GFAS is available at https://ads.atmosphere.copernicus.eu/datasets/cams-global-fire-emissions-gfas?tab=download. The GFED emissions can be accessed from https://www.globalfiredata.org/data.html. The boundary files can be accessed from https://www.naturalearthdata.com/. The data for generating the main figures are provide in the Source Data file. The CESM2 data generated in this study have been deposited in Figshare: https://doi.org/10.6084/m9.figshare.30984097.

Code Availability

The original CESM2 model code is available from https://www.cesm.ucar.edu/models/cesm2. The code for the updated stratospheric chemistry scheme used in this study can be found at Figshare: https://doi.org/10.6084/m9.figshare.30984097.

References

1. Caldwell, M.M., Flint, S.D. Stratospheric ozone reduction, solar UV-B radiation and terrestrial ecosystems. *Clim Change* **28**, 375-394 (1994).
2. Neale, R.E., Barnes, P.W., Robson, T.M., et al. Environmental effects of stratospheric ozone depletion, UV radiation, and interactions with climate change: UNEP Environmental Effects Assessment Panel, Update 2020. *Photoch Photobio Sci* **20**, 1-67 (2021).
3. Bernath, P., Boone, C., Crouse, J. Wildfire smoke destroys stratospheric ozone. *Science* **375**, 1292-1295 (2022).
4. Solomon, S., Stone, K., Yu, P., et al. Chlorine activation and enhanced ozone depletion induced by wildfire aerosol. *Nature* **615**, 259-264 2023.
5. Damany-Pearce, L., Johnson, B., Wells, A. et al. Australian wildfires cause the largest stratospheric warming since Pinatubo and extends the lifetime of the Antarctic ozone hole. *Sci Rep* **12**, 12665 (2022).
6. Yu, P., Davis, S.M., Toon, O.B., et al. Persistent stratospheric warming due to 2019–2020 Australian wildfire smoke. *Geophys Res Lett*, **48**, e2021GL092609 (2021).
7. Ma, C., Su, H., Lelieveld, J., et al. Smoke-charged vortex doubles hemispheric aerosol in the middle stratosphere and buffers ozone depletion. *Sci Adv* **10**, eadn3657 (2024).
8. Friedel, M., Chiodo, G., Stenke, A. et al. Springtime arctic ozone depletion forces northern hemisphere climate anomalies. *Nat Geosci* **15**, 541–547 (2022).
9. Ohneiser, K., Ansmann, A., Chudnovsky, A., et al. The unexpected smoke layer in the High Arctic winter stratosphere during MOSAiC 2019–2020. *Atmos Chem Phys* **21**, 15783-15808 (2021).
10. Ansmann, A., Ohneiser, K., Chudnovsky, A., et al. Ozone depletion in the Arctic and Antarctic stratosphere induced by wildfire smoke. *Atmos Chem Phys* **22**, 11701-11726 (2022).

11. Zhong, Q., Schutgens, N., Veraverbeke, S. et al. Increasing aerosol emissions from boreal biomass burning exacerbate Arctic warming. *Nat Clim Chang* **14**, 1275-1281 (2024).
12. Blanchard-Wrigglesworth, E., DeRepentigny, P., Frierson, D.M. Increasing boreal fires reduce future global warming and sea ice loss. *Proc Nat Acad Sci USA* **122**, e2424614122 (2025).
13. Zamora, L.M., Kahn, R.A., Cubison, M.J., et al. Aircraft-measured indirect cloud effects from biomass burning smoke in the Arctic and subarctic. *Atmos Chem Phys* **16**, 715-738 (2016).
14. DeRepentigny, P., Jahn, A., Holland, M.M., et al. Enhanced simulated early 21st century Arctic sea ice loss due to CMIP6 biomass burning emissions. *Sci Adv* **8**, eabo2405 (2022).
15. Lawrence, Z.D., Perlwitz, J., Butler, A.H., et al. The remarkably strong Arctic stratospheric polar vortex of winter 2020: Links to record-breaking Arctic oscillation and ozone loss. *J Geophys Res Atmos* **125**, e2020JD033271 (2020).
16. Dameris, M., Loyola, D.G., Nützel, M., et al. Record low ozone values over the Arctic in boreal spring 2020. *Atmos Chem Phys* **21**, 617-633 (2021).
17. Butchart, N. The brewer-dobson circulation. *Rev Geophys* **52**, 157-184 (2014).
18. Descals, A., Gaveau, D.L., Verger, A., et al. Unprecedented fire activity above the Arctic Circle linked to rising temperatures. *Science* **378**, 532-537 (2022).
19. Danabasoglu, G., Lamarque, J.F., Bacmeister, J., et al. The community earth system model version 2 (CESM2). *J Adv Model Earth Syst* **12**, e2019MS001916 (2020).
20. Waythomas, C.F., Scott, W.E., Prejean, S.G., et al. The 7–8 August 2008 eruption of Kasatochi Volcano, central Aleutian Islands, Alaska. *J Geophys Res Solid Earth* 1**15**, B00B06 (2010).
21. Jégou, F., Berthet, G., Brogniez, C., et al. Stratospheric aerosols from the Sarychev volcano eruption in the 2009 Arctic summer. *Atmos Chem Phys* **13**, 6533-6552 (2013).
22. Cai, Z., Griessbach, S., Hoffmann, L. Improved estimation of volcanic SO2 injections from satellite retrievals and Lagrangian transport simulations: the 2019 Raikoke eruption. *Atmos Chem Phys* **22**, 6787–6809 (2022).
23. Schuster, G.L., Dubovik, O., Holben, B.N. Angstrom exponent and bimodal aerosol size distributions. *J Geophys Res Atmos* **111**, D07207, (2006).
24. Ansmann, A., Veselovskii, I., Ohneiser, K., Chudnovsky, A. Comment on "Stratospheric Aerosol Composition Observed by the Atmospheric Chemistry Experiment Following the 2019 Raikoke Eruption" by Boone et al. *J Geophys Res Atmos* **129**, e2022JD038080 (2024).
25. Niemeier, U., Schmidt, H. Changing transport processes in the stratosphere by radiative heating of sulfate aerosols. *Atmos Chem Phys* **17**, 14871-14886 (2017).
26. Rex, M., Salawitch, R.J., von der Gathen, P., et al. Arctic ozone loss and climate change. *Geophys Res Lett* **31**, L04116 (2004).
27. Manney G.L., Livesey, N.J., Santee, M.L., et al. Record-Low Arctic Stratospheric Ozone in 2020: MLS Observations of Chemical Processes and Comparisons With Previous Extreme Winters. *Geophys Res Lett* **47**, e2020GL089063 (2020).
28. Weber, M., Arosio, C., Feng, W., et al. The Unusual Stratospheric Arctic Winter 2019/20: Chemical Ozone Loss From Satellite Observations and TOMCAT Chemical Transport Model. *J Geophys Res Atmos* **126**, e2020JD034386 (2021).
29. van Der Werf, G.R., Randerson, J.T., Giglio, L., et al. Global fire emissions estimates during 1997–2016. *Earth Syst Sci Data* **9**, 697-720 (2017).
30. Stone, K.A., Solomon, S., Kinnison, D.E. Mills, M.J. On recent large Antarctic ozone holes and ozone recovery metrics. *Geophys Res Lett* **48**, e2021GL095232 (2021).
31. Manney, G.L., Millán, L.F., Santee, M.L., et al. Signatures of Anomalous Transport in the 2019/2020 Arctic Stratospheric Polar Vortex *J Geophys Res Atmos* **127**, e2022JD037407 (2022).
32. Qin, Y., Gu, S., Dou, X., et al. Contributions of Early- and Middle-Winter Perturbations at Higher Altitudes to Late-Winter Anomalously Strong Arctic Polar Vortex in the Lower Stratosphere. *J Geophys Res Atmos* **127**, e2022JD037542 (2022).
33. Fromm, M., Servranckx, R., Stocks, B.J. et al. Understanding the critical elements of the pyrocumulonimbus storm sparked by high-intensity wildland fire. *Commun Earth Environ* **3**, 243 (2022).
34. Zhong, Q., Schutgens, N., Van Der Werf, G., et al. Satellite-based evaluation of AeroCom model bias in biomass burning regions. Atmos Chem Phys **22**, 1-47 (2022).
35. Koffi, B., Schulz, M., Bréon, F.M., et al. Evaluation of the aerosol vertical distribution in global aerosol models through comparison against CALIOP measurements: AeroCom phase II results. *J Geophys Res Atmos* **121**, 7254-

7283 (2016).
36. Senande-Rivera, M., Insua-Costa, D., Miguez-Macho, G. Spatial and temporal expansion of global wildland fire activity in response to climate change. *Nat Commun* **13**, 1208 (2022).
37. Scholten, R.C., Veraverbeke, S., Chen, Y. et al. Spatial variability in Arctic–boreal fire regimes influenced by environmental and human factors. *Nat Geosci* **17**, 866-873 (2024).
38. Westervelt, D.M., Mascioli, N.R., Fiore, A.M., et al. Local and remote mean and extreme temperature response to regional aerosol emissions reductions. *Atmos Chem Phys* **20**, 3009-3027 (2020).
39. Meehl, G.A., Senior, C.A., Eyring, V., et al. Context for interpreting equilibrium climate sensitivity and transient climate response from the CMIP6 Earth system models. *Sci Adv* **6**, eaba1981 (2020).
40. Boone, C.D., Bernath, P.F., Labelle, K., Crouse, J. Stratospheric Aerosol Composition Observed by the Atmospheric Chemistry Experiment Following the 2019 Raikoke Eruption. *J Geophys Res Atmos* **127**, e2022JD036600 (2022).
41. Kar, J., Lee, K.-P., Vaughan, M.A., et al. CALIPSO level 3 stratospheric aerosol profile product: version 1.00 algorithm description and initial assessment. *Atmos Meas Tech* **12**, 6173-6191 (2019).
42. Taha, G., Loughman, R., Zhu, T., et al. OMPS LP Version 2.0 multi-wavelength aerosol extinction coefficient retrieval algorithm. *Atmos Meas Tech* **14**, 1015–1036 (2021).
43. Chen, Z., Bhartia, P.K., Torres, O., et al. Evaluation of the OMPS/LP stratospheric aerosol extinction product using SAGE III/ISS observations. *Atmos Meas Tech* **13**, 3471-3485 (2020).
44. Platnick, S., et al., 2015. MODIS Atmosphere L3 Daily Product. NASA MODIS Adaptive Processing System, Goddard Space Flight Center, USA: http://dx.doi.org/10.5067/MODIS/MOD08_D3.061
45. Davis, S.M., Rosenlof, K.H., Hassler, B., et al. The Stratospheric Water and Ozone Satellite Homogenized (SWOOSH) database: a long-term database for climate studies. *Earth Syst Sci Data* **8**, 461-490 (2016).
46. Hersbach, H., Bell, B., Berrisford, P., et al. (2023): ERA5 monthly averaged data on pressure levels from 1940 to present. Copernicus Climate Change Service (C3S) Climate Data Store (CDS), DOI: 10.24381/cds.6860a573 (Accessed on 20-12-2024).
47. Kaiser, J.W., Heil, A., Andreae, M.O., et al. Biomass burning emissions estimated with a global fire assimilation system based on observed fire radiative power. *Biogeosciences* **9**, 527-554 (2012).
48. Gettelman, A., Mills, M.J., Kinnison, D.E., et al. The whole atmosphere community climate model version 6 (WACCM6). *J Geophys Res Atmos* **124**, 12380-12403 (2019).

Acknowledgements

This work is supported by the National Natural Science Foundation of China (NSFC 42477392), the NSFC Excellent Young Scientists Fund Program (Overseas), and Fundamental and Interdisciplinary Disciplines Breakthrough Plan of the Ministry of Education of China (JYB2025XDXM909). The CESM2 simulations were carried out at National Supercomputer Center in Tianjin, and the calculations were performed on Tianhe new generation supercomputer. The contribution of SV was supported by the European Research Council (ERC) through a Consolidator grant under the European Union's Horizon 2020 research and innovation program (grant no. 101000987). We acknowledge the valuable suggestions from Prof. Nick Schutgens (Vrije Universiteit Amsterdam) and Prof. Guido van der Werf (Wageningen University & Research).

Author Contributions

Q.Z. designed this study, performed the model experiments of CESM2, conducted the data analysis, and wrote the initial manuscript. S.V. provided important aspects on boreal fire dynamics. P.Y.

offered advice on stratospheric chemistry. J.M. and S.T. provided scientific advice and valuable comments on the atmospheric dynamics. All authors contributed to reviewing and improving the final version of the manuscript.

Competing Interests

The authors declare no competing interests.

Figure Captions

Fig. 1 Observed anomalies for Arctic stratospheric aerosols and ozone (O_3). (a) Monthly anomalies of stratospheric aerosol optical depth (SAOD) from 2006 to 2021 based on the Cloud-Aerosol Lidar with Orthogonal Polarization (CALIOP) observations. Data for three years with large SAOD anomalies are labelled in different colours. The embedded map shows the average SAOD anomaly from August to October in 2019, with solid black line indicating the Arctic area (> 60°N). (b) Monthly anomaly of total column ozone (TCO) from 1979 to 2024 based on NASA Ozone Watch (https://ozonewatch.gsfc.nasa.gov/). The blue line indicates 2020 data. The embedded map shows the average TCO anomaly from February to April in 2020 based on the Ozone Mapping and Profiler Suite (OMPS) data. (c1-c3) Vertical profiles of aerosol extinction anomaly from 2006 to 2021 for August (Aer-Aug), September (Aer-Sep), and October (Aer-Oct), respectively. (d1-d3) Vertical profiles of O_3 mixing ratio anomaly in the Arctic stratosphere from 2000 to 2023 for February (O_3-Feb), March (O_3-Mar), and April (O_3-Apr), respectively.

Fig. 2 Modelled ozone (O_3) anomalies induced by stratospheric biomass burning aerosols (SBBA) over the Arctic. (a) Monthly anomalies of modelled total column ozone (TCO) and stratospheric aerosol optical depth (SAOD). Data are shown from June 2019 to May 2020. TCO results are shown as the difference between FIRE19 and CLIM (red solid line) and between CLIM and NOBB runs (red dashed line). The shaded area indicates interquartile ranges of the O_3 anomaly from the 20 ensemble members considering the overall impacts of SBBA. The differences between FIRE19 and CLIM are further divided into the impacts of dynamic (in orange) and chemistry (in blue, see Methods). The results for CLIM and NOBB are not specifically for the 2019–2020 period, but instead averaged over the 24-year (2000–2023) simulations to provide a climatology baseline. For comparison, the modelled anomalies of SAOD are shown as lines with symbols. (b) Anomalies of vertical profiles for O_3 mixing ratio in the Arctic during 2020 spring (February–April). (c-e) Modelled spatial distributions of TCO anomalies between FIRE19 and CLIM in 2020 spring, considering the overall (c), dynamical (d), and chemical impacts of SBBA (e). The stippling indicates significant anomalies at 0.1 level. The upper-right numbers show the average TCO anomalies caused by SBBA over the Arctic.

Fig. 3 Spatiotemporal anomalies of the Arctic ozone (O_3) in response to stratospheric biomass burning aerosols (SBBA). (a_1) Monthly anomalies of the Arctic O_3 mixing ratio affected by SBBA from May 2019 to June 2020. Results are shown as differences between FIRE19 and CLIM simulations for overall SBBA impacts (Methods). The vertical lines indicate the three stages of O_3 evolution. (a_2-a_4) Vertical profiles of anomalies in O_3 mixing ratio averaged over Stages-1, 2, and 3, respectively. (b_1-b_4, c_1-c_4) The same as (a_1-a_4) but for the dynamic and chemistry impacts of SBBA, respectively. (d_1, e_1) Anomalies in temperature (d_1) and potential vorticity (e_1) averaged over Stage-3 at 20 hPa height caused by dynamical impacts of SBBA. (d_2-d_4, e_2-e_4) Vertical profiles of anomalies due to dynamical impacts averaged over three stages for temperature (Temp.) and potential vorticity (PV), respectively. The stippling indicates significant anomalies between FIRE19 and CLIM simulations at 0.1 level.

Fig. 4 Observed stratospheric aerosol optical depth (SAOD) and circulation patterns in mid-to-high latitudes in Northern Hemisphere. (a, b) Daily series of SAOD in the Arctic (> 60°N) and middle latitudes (40–60°N) from 2012 to 2023 based on the Ozone Mapping and Profiler Suite (OMPS) observations. Data for three years (2019, 2020, 2021) with intense BBA emissions from Siberia (Fig. S29) are shown in different colours. The embedded maps show the monthly mean SAOD observation for July 2019, during which substantial SAOD within the Arctic is observed. The shaded areas indicate the focused regions in each diagram. (c–e) Anomalies of geopotential (background maps) and wind fields (arrows), as well as locations of extreme fire events (red dots) in July for 2019, 2020, and 2021. (f) 2003–2023 averages for geopotential and wind field, as well as the combination of all extreme fires (red dots). The data in 2019–2021 are excluded from this climatology. In (c–f), fires with fire radiative power higher than 100 MW per 0.1-degree grid-cell on a daily basis are selected as extreme events. The geopotential and wind fields are shown for 300 hPa level to present the circulation patterns of the upper troposphere/lower stratosphere.

Editorial Summary

Stratospheric biomass burning aerosols can impact ozone through multiple pathways. This work shows that the 2019 fire aerosols caused a net increase in Arctic ozone, primarily through stratospheric heating and enhanced poleward ozone transport.

Peer review information: *Nature Communications* thanks the anonymous reviewers for their contribution to the peer review of this work. A peer review file is available.

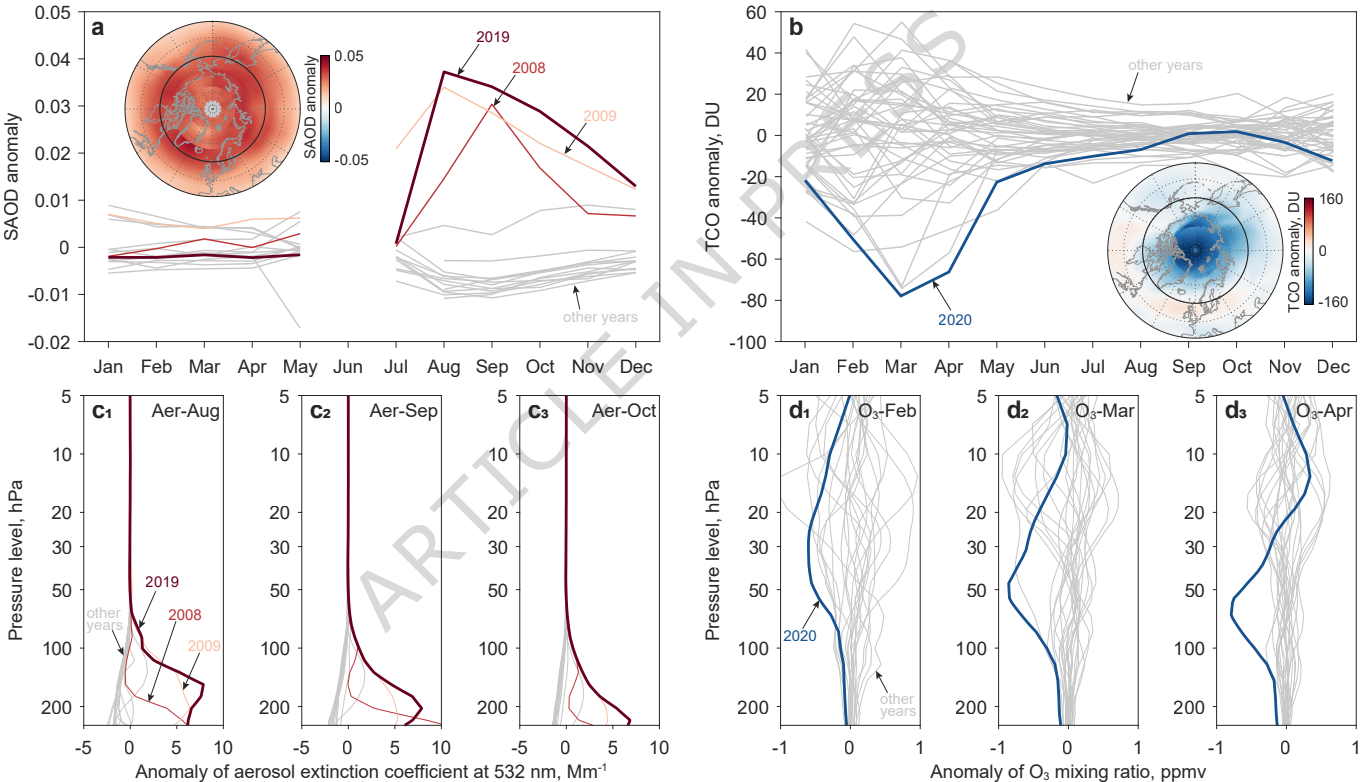

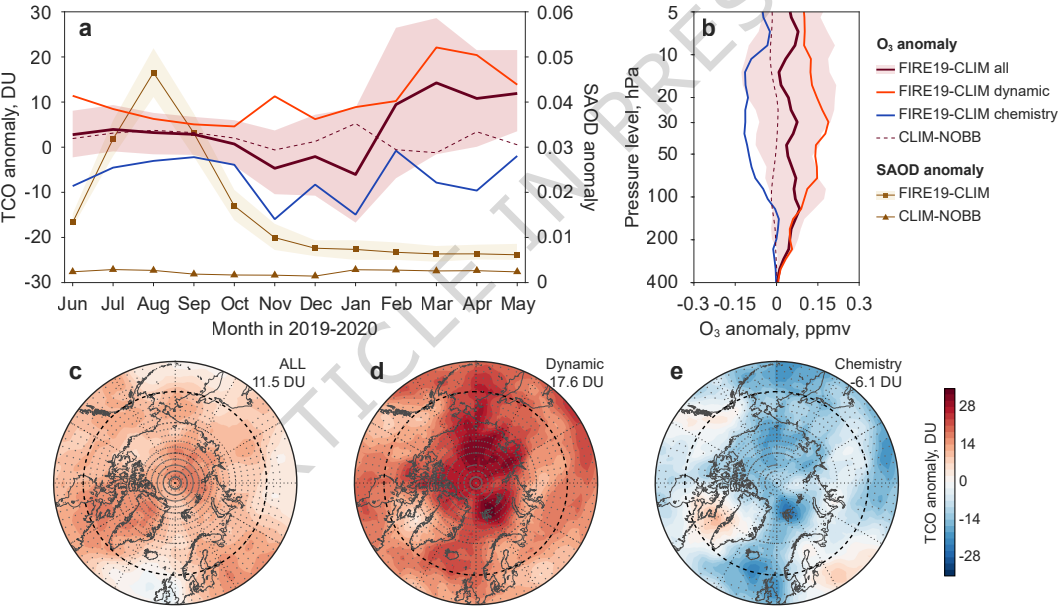

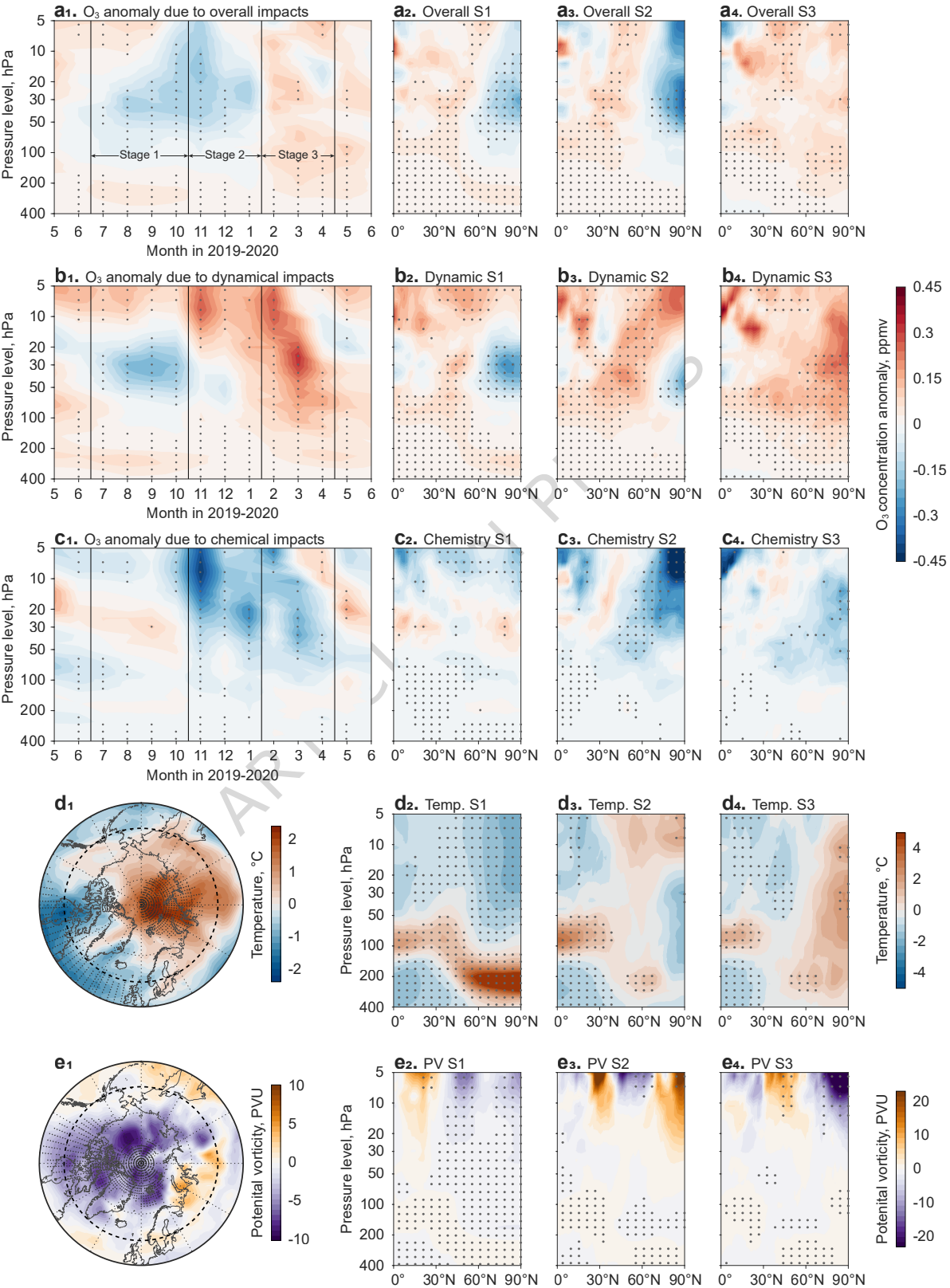

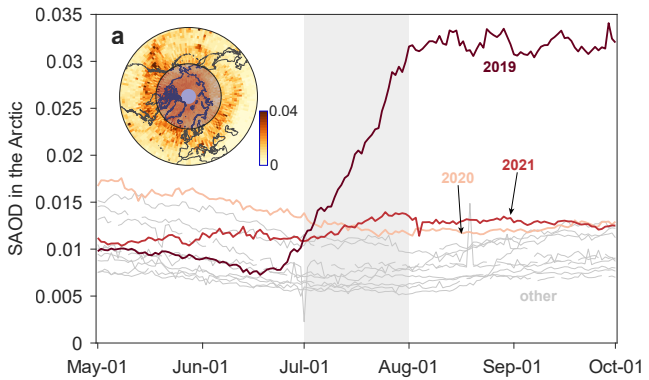
a
SAOD in the Arctic
0.035
0.03
0.025
0.02
0.015
0.01
0.005
0
0.04
0
2019
2020
2021
other
May-01
Jun-01
Jul-01
Aug-01
Sep-01
Oct-01

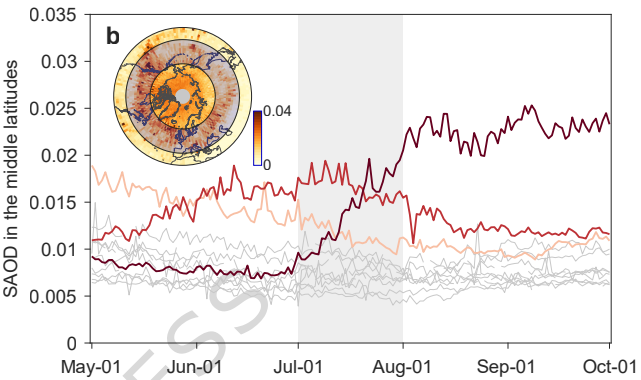
b
SAOD in the middle latitudes
0.035
0.03
0.025
0.02
0.015
0.01
0.005
0
0.04
0
May-01
Jun-01
Jul-01
Aug-01
Sep-01
Oct-01

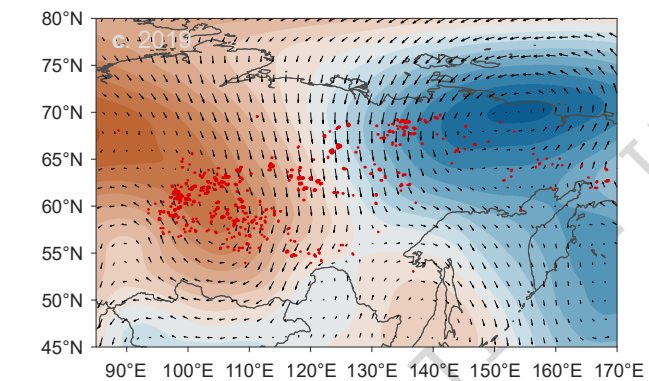
c. 2019
80°N
75°N
70°N
65°N
60°N
55°N
50°N
45°N
90°E
100°E
110°E
120°E
130°E
140°E
150°E
160°E
170°E

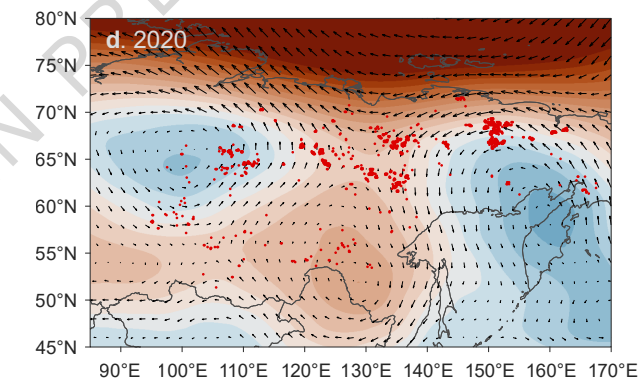
d. 2020
80°N
75°N
70°N
65°N
60°N
55°N
50°N
45°N
90°E
100°E
110°E
120°E
130°E
140°E
150°E
160°E
170°E

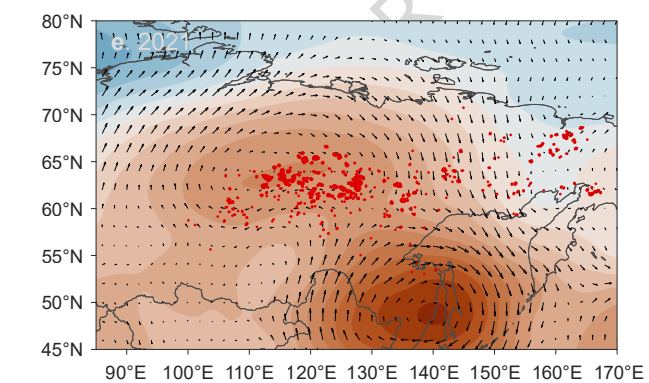
e. 2021
80°N
75°N
70°N
65°N
60°N
55°N
50°N
45°N
90°E
100°E
110°E
120°E
130°E
140°E
150°E
160°E
170°E

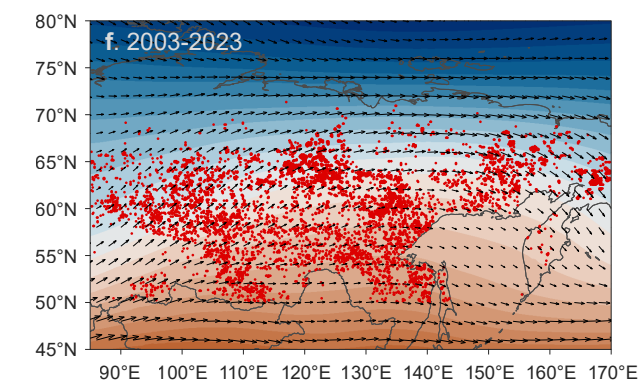
f. 2003-2023
80°N
75°N
70°N
65°N
60°N
55°N
50°N
45°N
90°E
100°E
110°E
120°E
130°E
140°E
150°E
160°E
170°E

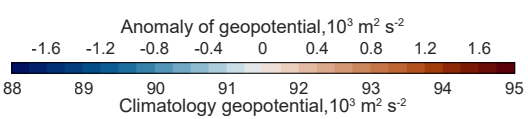
Anomaly of geopotential,10³ m² s⁻²
-1.6
-1.2
-0.8
-0.4
0
0.4
0.8
1.2
1.6
88
89
90
91
92
93
94
95
Climatology geopotential,10³ m² s⁻²